Chemistry Letters

http://www.csj.jp/journals/chem-lett/

Vol.33 No.9
September, 2004

CMLTAG
ISSN 0366-7022

Highlight Review

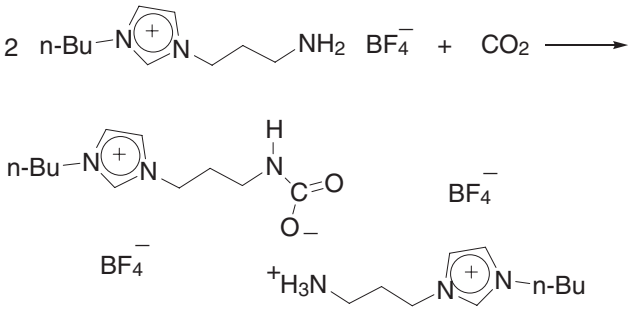

Task-specific ionic liquids are a unique subclass of ionic liquids which possess a potential spectrum of utility extending far beyond that likely for more conventional IL. By virtue of their covalently tethered functional groups, these unique salts can act not only as solvents but as catalysts and reagents in an array of synthetic, separations, and electrochemical applications.

Letter

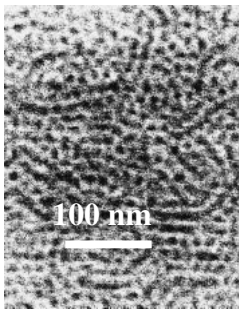

1080 **CO_2 Sensing Properties of La-loaded SnO_2 Thin Films Prepared by Sputtering**

The excellent detection sensitivity to CO_2 in air was achieved by use of La_2O_3-loaded SnO_2 sensors prepared using sputtering method.

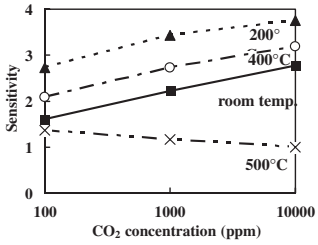

Hiroshi Sakama, Shinji Saeki, Atsushi Ono, Noriya Ichikawa, Atsushi Tanokura, Hiroshi Uetsuka, and Hiroshi Onishi

1082 **Unprecedented Sequential Deprotonation of Ruthenium–Aqua Framework Affording Ruthenium–Oxo–Dithiolene Complex**

Introduction of dithiolene ligand into ruthenium–aqua–terpyridyl systems remarkably enhances acidity of the coordinated aqua ligand to dissociate two protons without any oxidants and changes its neutral oxo form only by pH gradient.

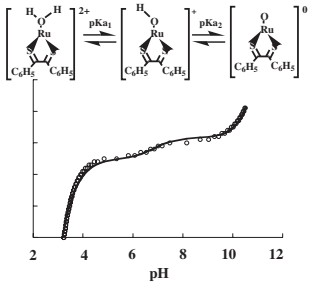

Hideki Sugimoto, Kazunobu Sato, Takeji Takui, and Koji Tanaka

1084 **Conversion of 3-*O*-Substituted 1,2-Dibromoalkanes into 2-Bromo-1-alkenes by the Selective Elimination: Its Application to Total Synthesis of 12-Oxygenated Tremetones**

Synthesis of 2-bromo-1-alkenes has been accomplished in good yields from 3-aryloxy or 3-acyloxy-1,2-dibromoalkanes by regioselective elimination reactions. The natural tremetone derivatives were successfully synthesized by utilizing the elimination reaction.

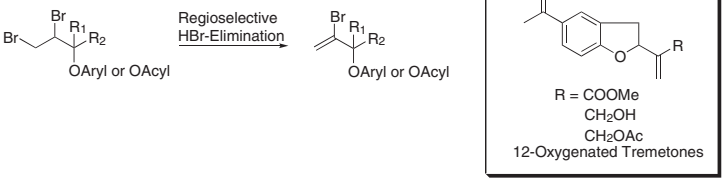

Tadaaki Ohgiya and Shigeru Nishiyama

1086 **Heptakis(2,3-di-*O*-carboxymethyl)-β-cyclodextrin as a pH-sensitive Host**

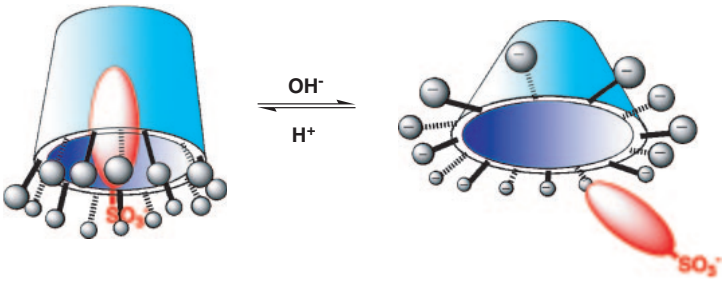

Koji Kano, Yasuhiro Horiki, Takahiro Mabuchi, and Hiroaki Kitagishi

1088 **Template-free Growth of Vertically Aligned CdS Nanowire Array Exhibiting Good Field Emission Property**

A novel template-free solvothermal route was successfully designed to fabricate single crystal vertically aligned CdS nanowire array, which showed good field emission property.

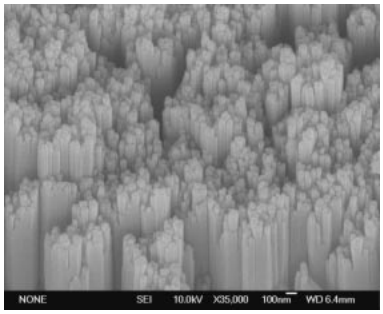

Qun Tang, Xihong Chen, Ting Li, Aiwu Zhao, Yitai Qian, Dapeng Yu, and Weichao Yu

1090 **Excitation Wavelength Dependence of Solvation Dynamics in a Water Pool of a Reversed Micelle**

Taku Satoh, Hiroaki Okuno, Keisuke Tominaga, and Kankan Bhattacharyya

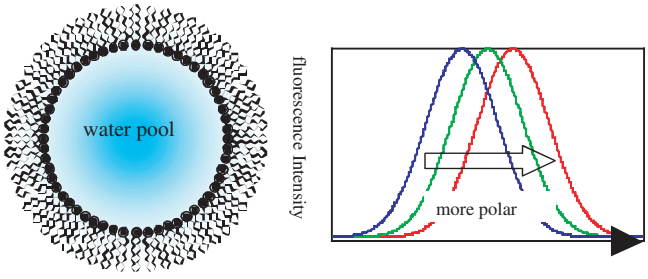

1092 **A Novel Photosensitizer of Palladium(II) Phthalocyanine Tetrasulfonate for Chlorophenol Oxidation under Visible Light Irradiation**

Meiqin Hu, Yiming Xu, and Zhigang Xiong

The title complex has been found to exhibit high quantum yield of singlet oxygen generation, and is highly efficient and stable to initiate mineralization of chlorophenols in water under visible light irradiation.

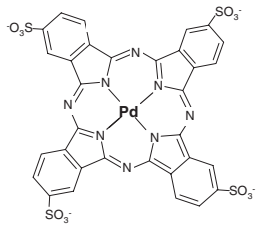

Φ ($^1O_2$) = 0.87
in DMF at λ = 606 nm

1094 **Solution Properties of a Novel Polysaccharide Derivative**

Takeshi Ihara, Tohru Nishioka, Hiroshi Kamitani, and Tomohito Kitsuki

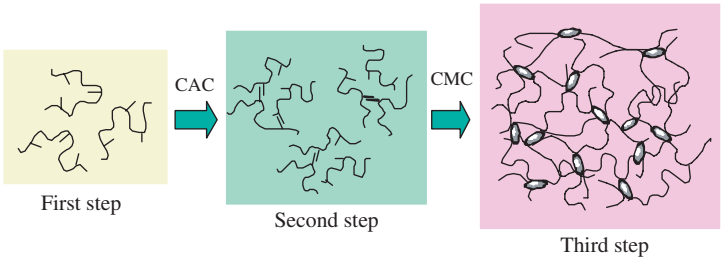

1096 **Novel Silver(I) and Copper(II) Complexes of Tetrakis(2-pyridyl)methane**

Kouzou Matsumoto, Masaki Kannami, and Masaji Oda

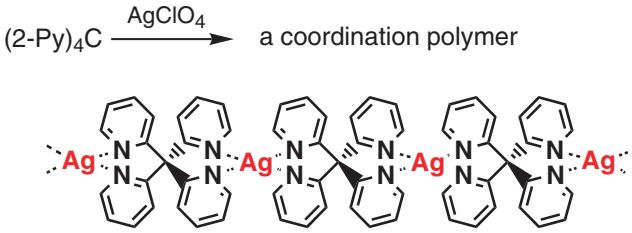

, and two kinds of complexes with Cu(II) ion.

1098 **Bis(tetrathiafulvaleno)octadehydro[20]annulene with Multi-functionality**

Masahiko Iyoda, Hideo Enozawa, and Yoshihiro Miyake

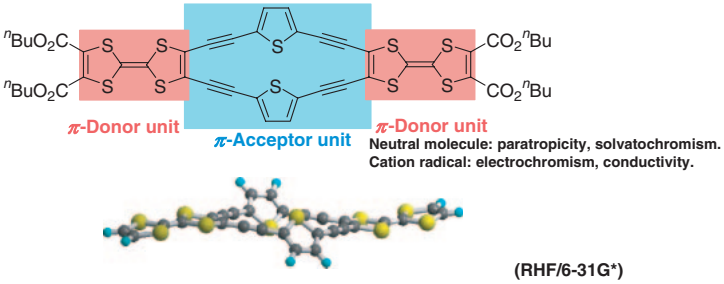

1100 **Molecular Design and Crystal Structures of Chiral Macrotricyclic Cage Amines**

Haruki Yoshida, Mitsunori Izumi, Naohito Ito, Kazuhiko Ichikawa, and Motoo Shiro

With a single asymmetric carbon, chiral (*R*)- and (*S*)-macrotricyclic cage amines (MCAs) have been synthesized. Each of their homochiral crystals consists of each single conformer characterized by asymmetric framework.

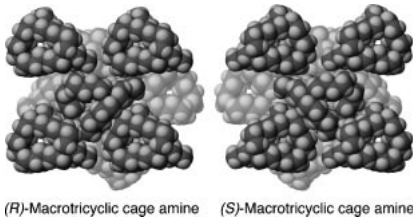

1102 **Bicontinuous Microemulsion-aided Synthesis of Mesoporous TiO_2**

Isamu Moriguchi, Yasuko Katsuki, Hirotoshi Yamada, Tetsuichi Kudo, and Taisei Nishimi

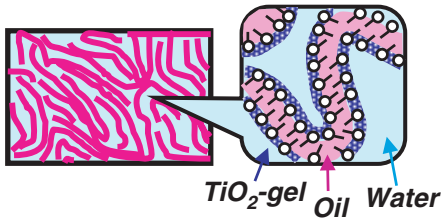

Bicontinuous microemulsion / TiO_2-gel composite

1104 **Preparation of $H_2Ti_4O_9$ with High Specific Surface Area**

Jinshu Wang, Shu Yin, and Tsugio Sato

$H_2Ti_4O_9$ nanocrystals precipitated by milling $K_2Ti_4O_9$ for 2 h and exfoliating in 1 M HCl followed by adjusting solution pH at 4 has nanosheets of lateral dimensions about 50 nm.

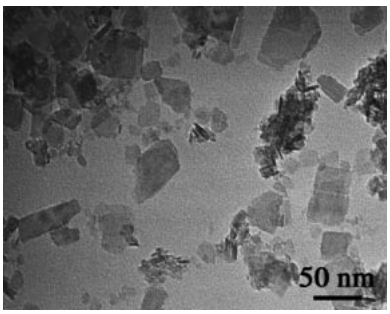

1106 **Synthesis of Magnetic Composite Particles of γ-Fe_2O_3@SiO_2 and the Control of the Structural Color of the Colloidal Crystal by Magnetic Fields**

Kazutoshi Kitajima, Toma Fujita, Norihito Sogoshi, and Seiichiro Nakabayashi

Color photographs of a composite magnetic colloidal crystal. Red spheres are ion-exchange resin beads. Structural color is seen in the middle of photographs and it changes from violet (the left photograph) to green (the right one) when magnetic fields are applied.

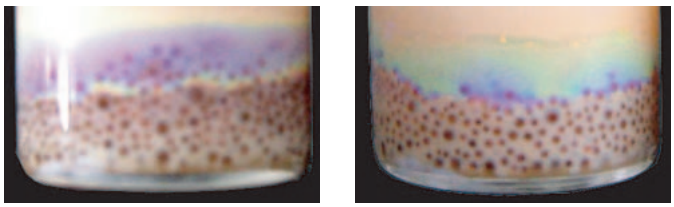

1108 **N-doped TiO_2 Nanotube with Visible Light Activity**

Hiromasa Tokudome and Masahiro Miyauchi

Nitrogen-doped TiO_2 nanotubes (anatase) were synthesized by a wet process. These nanotubes exhibited photocatalytic oxidation activity under visible light illumination.

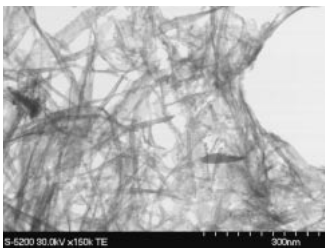

1110 **β-Hydride Elimination from α-Positioned Methyl Group of Bicyclic Zirconacyclopentanes Assisted by Aldehyde**

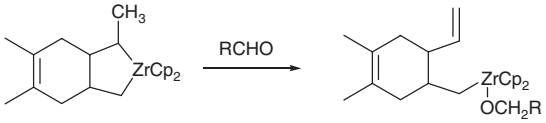

Zhenfeng Xi, Ruiyun Guo, Weixin Zheng, Hegen Zheng, Zhenqi Zhong, and Tamotsu Takahashi

1112 **Ion-exchangeable Layered Aminophenylsilica Prepared with Anionic Surfactant Templates**

A novel aminophenyl layered organosilica was synthesized using sodium dodecyl sulfate and *p*-aminophenyltrimethoxysilane utilizing the interaction between the surfactants and organofunctional groups of network-forming inorganic species.

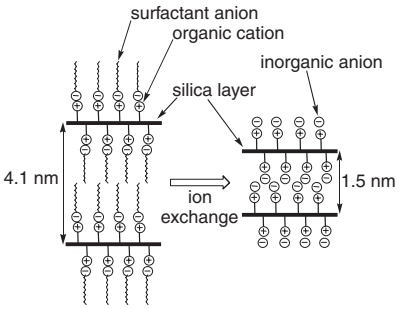

Ken Yao, Yusuke Imai, LiYi Shi, Eiichi Abe, Yoshio Adachi, Keiko Nishikubo, and Hiroshi Tateyama

1114 **CdS Nanowire-encapsulated, CdS Nanocrystals-enrobed Carbon Nanotubes Composites, and Their UV–vis Properties**

The fabrication of CdS nanowire-impregnated and CdS nanocrystal-coated carbon nanotube heterostructures is reported. These hybrid nanocomposites exhibit blue-shift absorption in UV–vis spectrum and provide various routes to nanotube composites.

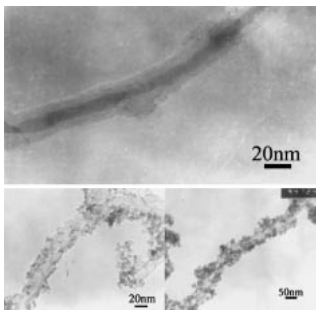

Linqin Jiang and Lian Gao

1116 **The Effect of Layered Sodium–Magadiite on the Photochromic Reversibility of Diarylethene Immobilized on Its Surfaces**

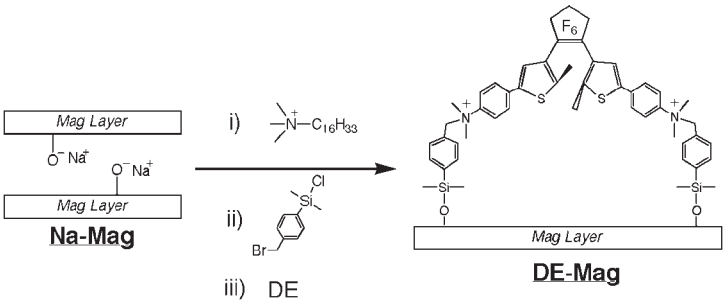

Itsuki Shindachi, Hiroshi Hanaki, Ryo Sasai, Tetsuya Shichi, Tatsuto Yui, and Katsuhiko Takagi

1118 **An Isothiouronium-derived Organized Monolayer at the Air–Water Interface: Design of Film-based Anion Sensor Systems for $H_2PO_4^-$**

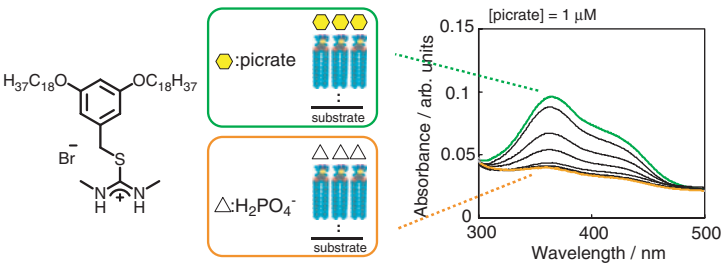

Yoshihiro Misawa, Yuji Kubo, Sumio Tokita, Hirokazu Ohkuma, and Hiroo Nakahara

1120 **Formation of Interconnected Macropores in Sm^{2+}-doped Silicate Glasses through Phase Separation: Fabrication of Photosensitive and Dielectrically Disordered Materials**

Koji Fujita, Shunsuke Murai, Yoshihiro Ohashi, Kazuki Nakanishi, and Kazuyuki Hirao

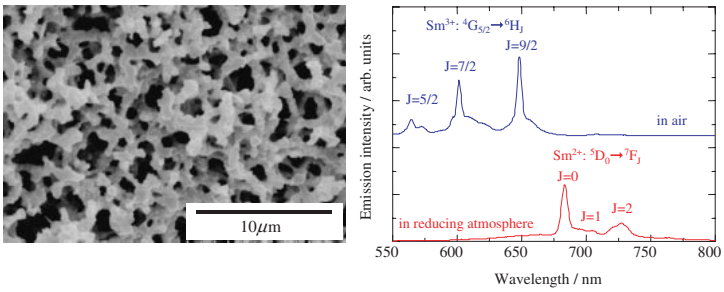

1122 **A Novel Synthetic Route to Layered Double Hydroxides Using Hexamethylenetetramine**

Nobuo Iyi, Taki Matsumoto, Yoshiro Kaneko, and Kenji Kitamura

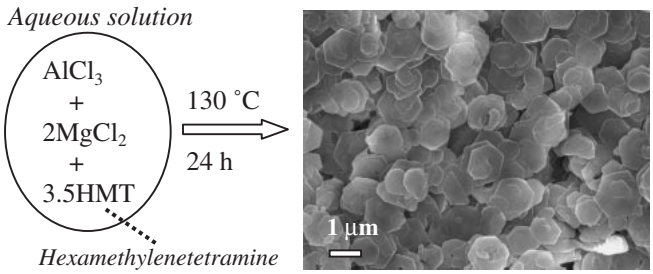

1124 **TICT Induced Fluorescence Color Change Actualized in an Organogel System**

Yuya Iwashita, Kazunori Sugiyasu, Masato Ikeda, Norifumi Fujita, and Seiji Shinkai

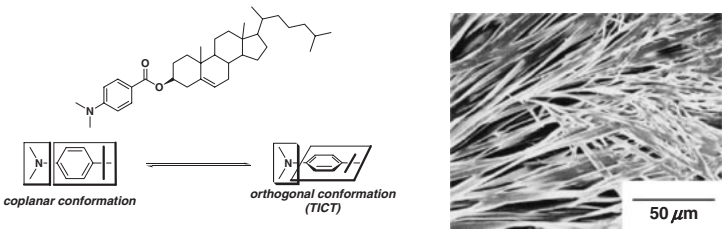

1126 **Hydrothermal Synthesis of [Al]-SSZ-24 from [Al]-Beta Zeolite ([Al]-BEA) as Precursors**

Hiroyoshi Maekawa, Yoshihiro Kubota, and Yoshihiro Sugi

Direct crystallization of aluminosilicate SSZ-24 ([Al]-SSZ-24) has been achieved for the first time by phase-transformation of beta zeolite ([Al]-**BEA**) in the presence of 16-methyl-16-azoniasparteine ($MeSPA^+$) as a structure-directing agent (SDA).

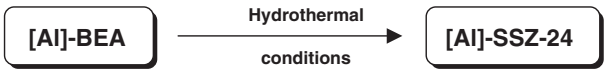

1128 **An Efficient Template Pathway to Synthesis of Ordered Metal Oxide Nanotube Arrays Using Metal Acetylacetonates as Single-Source Molecular Precursors**

Xiao-Ping Shen, Hong-Jiang Liu, Li Pan, Kang-Min Chen, Jian-Ming Hong, and Zheng Xu

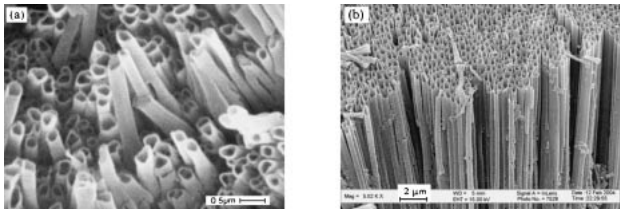

α-Fe_2O_3 and CuO nanotube arrays were obtained for the first time within the pores of the porous anodic alumina membranes by pyrolyzing $Fe(acac)_3$ and $Cu(acac)_2$, respectively.

1130 **Cluster Core Expansion through Incorporation of Transition-metal Fragments or an Alkyne Molecule into an Incomplete Cubane-type Fe_2RuS_4 Cluster**

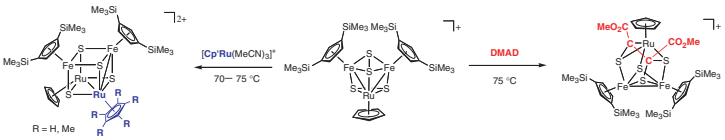

Masaaki Okazaki, Atsushi Sakuma, Hiromi Tobita, and Hiroshi Ogino

1132 **An Easy Route for the Synthesis of Ordered Three-Dimensional Large-Pore Mesoporous Organosilicas with *Im*-3*m* Symmetry**

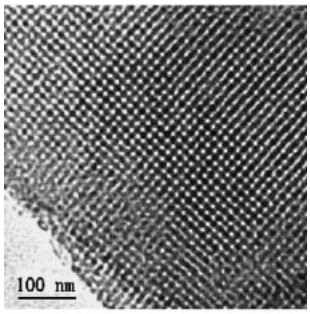

Zhendong Zhang, Bozhi Tian, Xiaoxia Yan, Shaodian Shen, Xiaoying Liu, Dehong Chen, Guangshan Zhu, Dongyuan Zhao, and Shilun Qiu

1134 **An Examination of the Gelation of Methacrylate Type Crosslinking Agents for the Preparation of Polymer Monolith with 3D Ordered Network Structures**

The unique macroporous gel with μm-sized pores homogeneously dispersed three dimensionally was formed in the gelation of glycerol dimethacrylate with toluene as diluent.

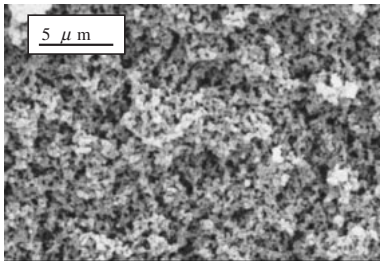

Hiroshi Aoki, Takuya Kubo, Yoshiyuki Watabe, Nobuo Tanaka, Tomohisa Norisuye, Ken Hosoya, and Kuniaki Shimbo

1136 **Preparation of Nanoparticles of $LiCoO_2$ Using Laser Ablation in Liquids**

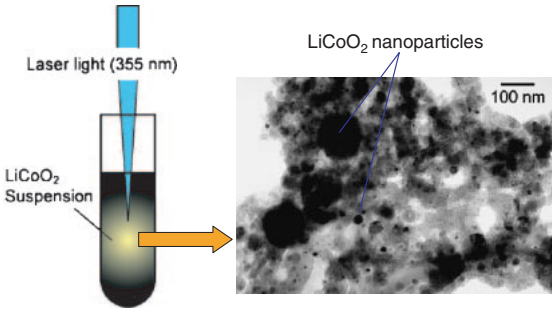

Takeshi Tsuji, Toshihiko Kakita, Taro Hamagami, Tetsuya Kawamura, Junichi Yamaki, and Masaharu Tsuji

1138 **Synthesis of Mesostructured Materials from K_2NbO_3F as Starting Material**

TEM image of the $K_2NbO_3F/C_{12}TMA$ complex.

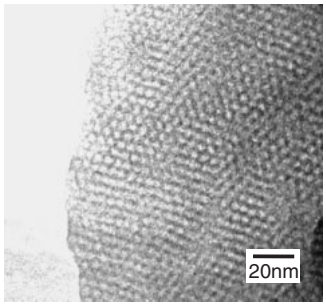

Masataka Ogasawara, Sumio Kato, Hiroshi Tsukidate, Takahiro Akaogi, Yoshio Moriya, and Shinichi Nakata

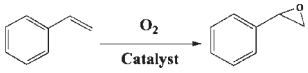

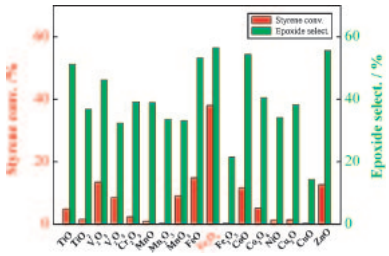

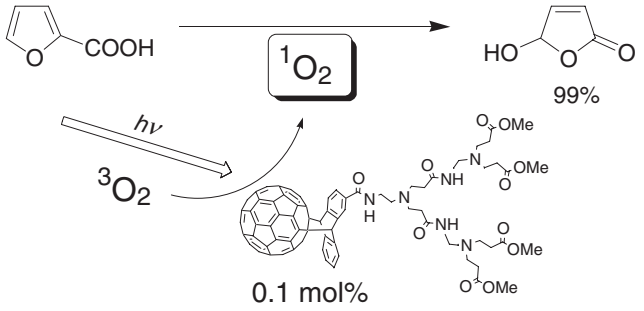

N,*N*′-dimethyl-*N*,*N*′-di-*n*-octyl-thiodiglycolamide (MOTDA) selectively extaracts Pd(II) from hydrochloric acid solution much faster than the convensional separation reagent, di-*n*-hexyl sulfide (DHS).

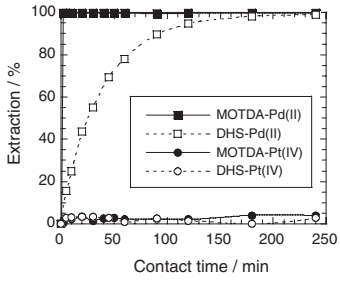

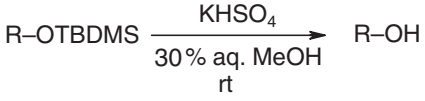

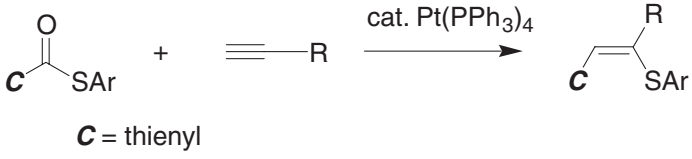

1150 **A Mild Reduction Route to PTFE Degradation at Low Temperature**

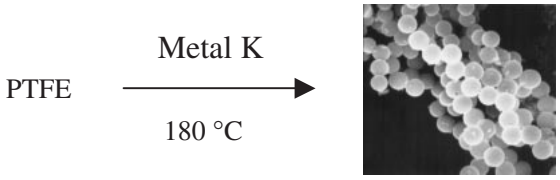

Guifu Zou, Dabin Yu, Changlong Jiang, Guangcheng Xi, Yitai Qian, and Houbo Zhang

Polytetrafluoroethylene (PTFE) has been degradated into non-crystalline carbon spheres by a benign method at low temperature

1152 **Significant Effect of Molecular Structure on Surface Relief Grating Formation for Novel Azobenzene-Based Photochromic Amorphous Molecular Materials**

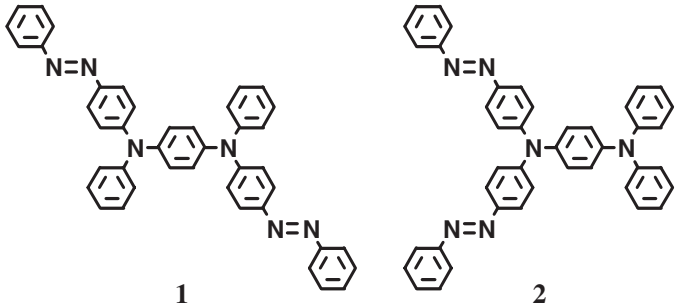

Hiromichi Ueda, Takahiro Tanino, Hiroyuki Ando, Hideyuki Nakano, and Yasuhiko Shirota

1154 **Dendrimer-Encapsulated Oligothiophenes**

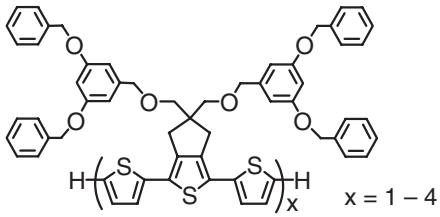

Tetsuo Otsubo, Shinpei Ueno, Kazuo Takimiya, and Yoshio Aso

1156 **Efficient Catalyst for Low Temperature Solid-Phase Imidization of Poly(amic acid)**

Thermal imidization of poly(amic acid) proceeded smoothly in the presence of 1 wt % of strong bases such as DABCO or DBU at 200 °C in a short time.

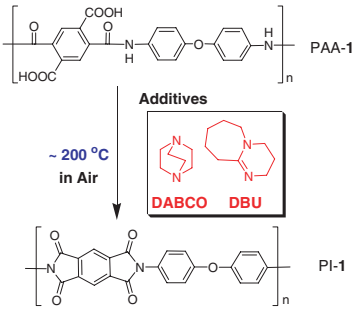

Ken-ichi Fukukawa, Yuji Shibasaki, and Mitsuru Ueda

1158 **Bio-template Synthesis of Uniform CdSe Nanoparticles Using Cage-shaped Protein, Apoferritin**

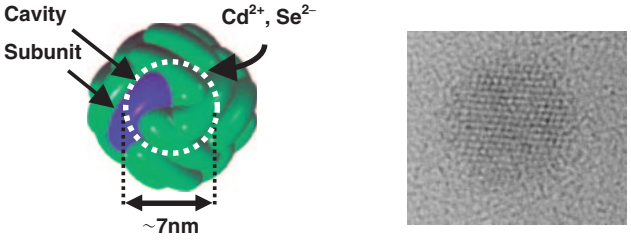

CdSe nanoparticles were synthesized in the cavity of the cage-shaped protein, apoferritin, by designing the slow chemical reaction system of Cd^{2+} and Se^{2-}.

Ichiro Yamashita, Junko Hayashi, and Masahiko Hara

1160 **Glucose Reduction Route Synthesis of Uniform Silver Nanowires in Large-scale**

Silver nanowires with average diameters of ~100 nm and lengths up to 800 μm were hydrothermally prepared in large scale by reducing silver nitrate with glucose in the presence of poly(vinyl alcohol) (PVA) at 160 °C.

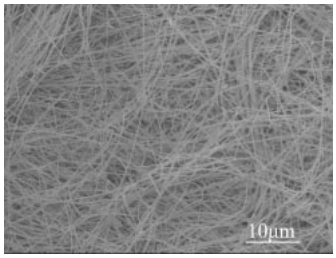

Zhenghua Wang, Xiangying Chen, Jianwei Liu, Meng Zhang, and Yitai Qian

1162 **Selective Synthesis of Wurtzite CdSe Nanorods and Zinc Blend CdSe Nanoparticals through Solvothermal Routes**

By simply changing the reactants' composition, highly crystallized wurtzite CdSe nanorods and zinc blend CdSe nanoparticles were selectively fabricated through a convenient solvothermal route.

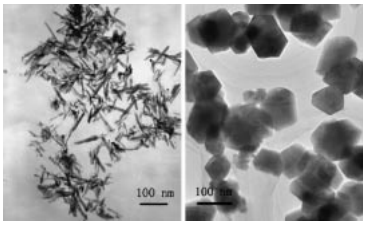

Yong Liu, Yao Xu, Jun-Ping Li, Bin Zhang, Dong Wu, and Yu-Han Sun

1164 **Degradation Pathways of Acetochlor by γ-Radiolysis**

Six radiolytic products of acetochlor under oxidative conditions and four under reductive conditions were separated and identified by a GCMS system. Based on this, degradation pathways of acetochlor by γ-irradiation were proposed.

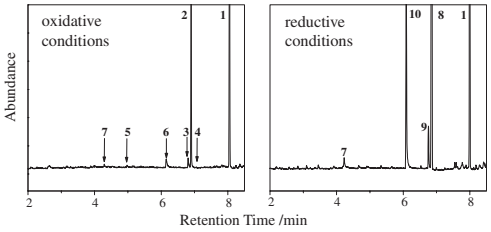

Shao-Yang Liu, You-Peng Chen, and Han-Qing Yu

1166 **Effects of Rhodium Addition to Mo/HZSM-5 Catalyst for Methane Dehydroaromatization**

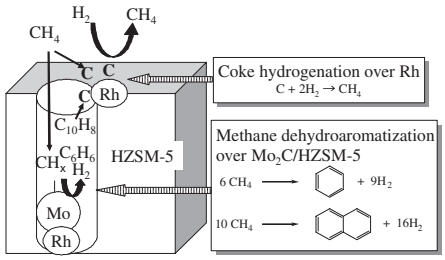

Ryoichi Kojima, Satoshi Kikuchi, and Masaru Ichikawa

Rhodium added Mo/HZSM-5 catalyst exhibited highly stable and active performances in the methane dehydroaromatization reaction with hydrogen addition due to the effective suppression of the coke deposition on the catalyst.

1168 **A Novel L-Proline Catalyzed Biginelli Reaction: One-Pot Synthesis of 3,4-Dihydropyrimidin-2(1*H*)-ones under Solvent-Free Conditions**

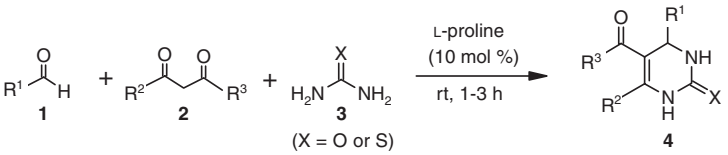

J. S. Yadav, S. Praveen Kumar, G. Kondaji, R. Srinivasa Rao, and K. Nagaiah

1170 **Characterization and Field-Effect Transistor Performance of Heterocyclic Oligomers Containing a Thiazolothiazole Unit**

Shinji Ando, Jun-ichi Nishida, Eiichi Fujiwara, Hirokazu Tada, Youji Inoue, Shizuo Tokito, and Yoshiro Yamashita

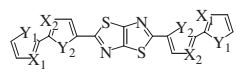

ZZFZZZ : X_1,X_2 = N / Y_1,Y_2 = S
ZTFZTZ : X_1 = N, X_2 = C / Y_1,Y_2 = S
FTFZTF : X_1,X_2 = C / Y_1 = O, Y_2 = S
FFFZFF : X_1,X_2 = C / Y_1,Y_2 = O

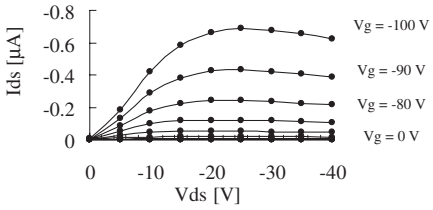

1172 **Low-voltage Organic Field-effect Transistors with a Gate Insulator of Ta_2O_5 Formed by Sputtering**

Heisuke Sakai, Yukio Furukawa, Eiichi Fujiwara, and Hirokazu Tada

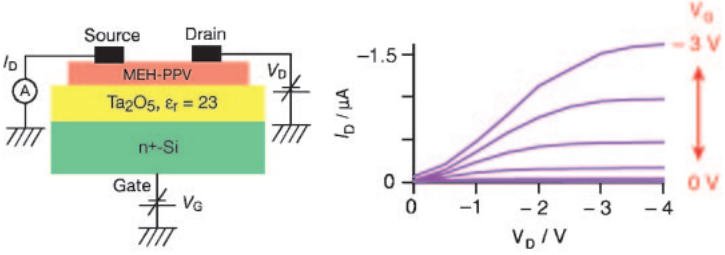

1174 **Synthesis, Structure, and Electron-Donating Ability of 2,2′:6′,2″-Dioxatriphenylamine and Its Sulfur Analogue**

Masato Kuratsu, Masatoshi Kozaki, and Keiji Okada

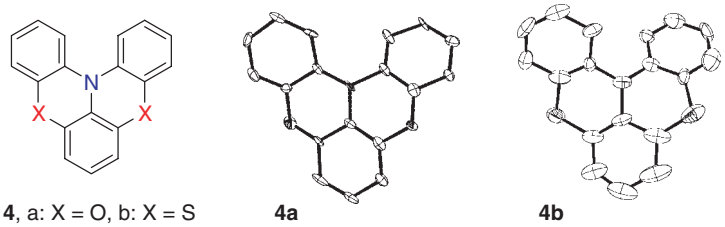

4, a: X = O, b: X = S **4a** **4b**

1176 **DFT Method Estimation of Standard Redox Potential of Metals**

Hisayoshi Kobayashi, Toshiko Miura, Yoshiki Shimodaira, and Akihiko Kudo

The DFT method calculation was carried out to evaluate standard redox potential for metal/metal cation systems. Utilizing the Born–Haber cycle and experimental values of the cohesive energy of metals, the root-mean-square deviation of calculated and experimental values was 0.29 V for 17 ions.

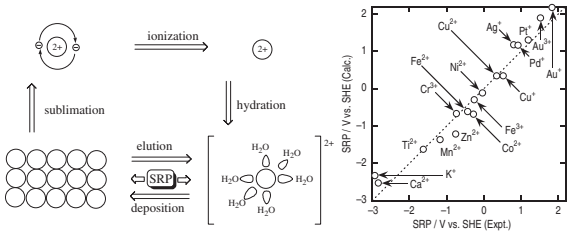

1178 **Peak Formation Due to Chemiluminescence Reaction through the Collapse of Laminar Flow Liquid–Liquid Interface in a Microreactor**

Kazuhiko Tsukagoshi, Keiichi Ikegami, Riichiro Nakajima, Kenichi Yamashita, and Hedeaki Maeda

A peak signal due to a chemiluminescence (CL) reaction in a microreactor consisting of a microchannel without sample plug formation is presented. A CL profile, including a peak signal, was observed by the collapse of the liquid–liquid interface based on laminar flow in the microchannel. Based on the measurements of peak height, Cu(II) was determined over the range of 20 nM–0.1 mM.

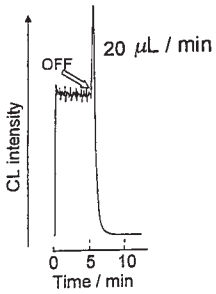

1180 **Tetrakis(trimethylsilylbutadiynyl)ethene, $C_{18}(SiMe_3)_4$: An Extended Two-Dimensional π-Conjugated System Consisting of Eighteen Carbon Atoms**

Takehiro Ozawa and Munetaka Akita

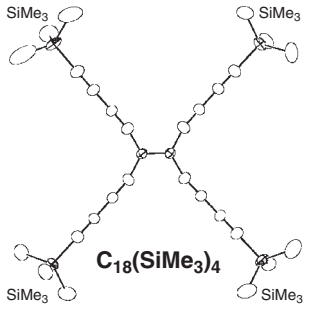

1182 **Fluorescent Property of Bulk- and Nanocrystals of Cyanide-bridged Eu(III)Co(III) Heteronuclear Coordination Polymer**

Nobuyuki Kondo, Arisa Yokoyama, Masato Kurihara, Masatomi Sakamoto, Mami Yamada, Mikio Miyake, Tetsu Ohsuna, Hiromichi Aono, and Yoshihiko Sadaoka

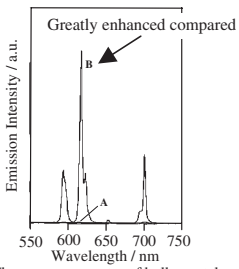

Fluorescence spectra of bulk crystals
A: $EuCl_3 \cdot 6H_2O$, B: $Eu[Co(CN)_6] \cdot 4H_2O$

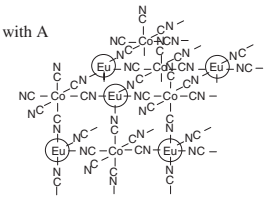

Fluorescene of bulk crystals was enhanced compared with $EuCl_3 \cdot 6H_2O$, whereas that of nanocrystals was little changed. These results were discussed considering the coordination surroundings around Eu(III) on the crystal surface.

1184 **Biselides A and B, Novel Macrolides from the Okinawan Ascidian Didemnidae sp.**

Toshiaki Teruya, Hiroki Shimogawa, Kiyotake Suenaga, and Hideo Kigoshi

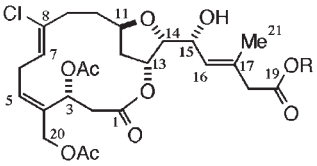

Biselide A R = H

Biselide B R =

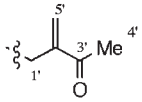

1186 **A Novel Open-framework Cerium Sulfate Hydrate: Synthesis and Characterization**

Ranbo Yu, Dan Wang, Yunfa Chen, Xianran Xing, Shintaro Ishiwata, Takashi Saito, and Mikio Takano

A novel open-framework cerium sulfate hydrate has been prepared from a hydrothermal system. The alternately arranged CeO_7 and SO_4 are connected to form a 3-D framework with eight-membered channel system.

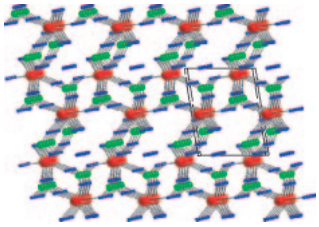

1188 **Cellulose Derivative-based Beads as Chiral Stationary Phase for HPLC**

Tomoyuki Ikai, Reiko Muraki, Chiyo Yamamoto, Masami Kamigaito, and Yoshio Okamoto

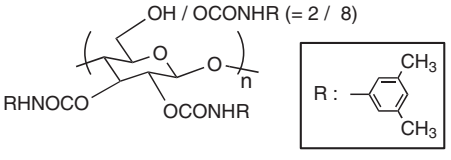

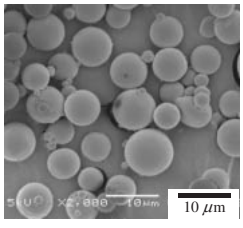

Cellulose Derivative-based Beads

1190 **Novel Donor–π–Acceptor Compounds Containing 1,3-Dithiol-2-ylidene and Tetracyanobutadiene Units**

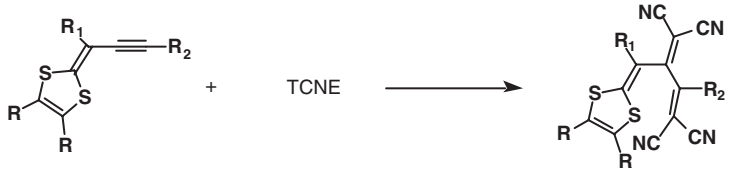

Yosuke Morioka, Naoto Yoshizawa, Jun-ichi Nishida, and Yoshiro Yamashita

1192 **Preparation of Nitriles from Primary Alcohols by a New Type of Oxidation-reduction Condensation Using 2,6-Dimethyl-1,4-benzoquinone and Diethyl Cyanophosphonate**

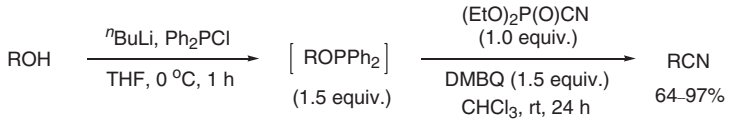

Teruaki Mukaiyama, Kouta Masutani, and Yoshiaki Hagiwara

1194 **Novel Way to Synthesize CuO Nanocrystals with Various Morphologies**

CuO nanocrystals with various morphologies have been prepared by a convenient hydrothermal decomposition route. The leaflike nanocrystals with the width and length in the range of 40–45 nm and 150–200 nm can be synthesized at the volume ratio of DMSO to water of 1:1.

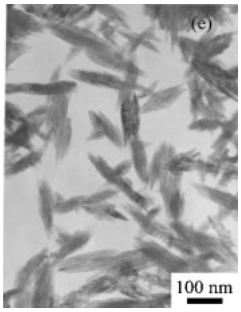

Rui Yang and Lian Gao

1196 **Photochemical Polar Addition of 1,1-Diphenylethene Using Photosensitive Surfactant in Stable Oil-in-Water Emulsion**

An aq. NaOH solution of the photosensitive surfactant **1** was mixed with 1,1-diphenylethene **2** to form a stable oil-in-water emulsion and excitation of the emulsion afforded the alcohol **3** in good yield without stirring. The photosensitive surfactant **1** works more efficiently in heterogeneous system (in water) than in homogeneous system (in organic solvent).

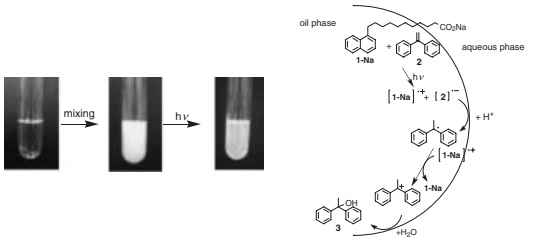

Yasuharu Yoshimi, Michiya Higuchi, Tatsuya Itou, and Minoru Hatanaka

1198 **Electrodepositing Redox Polymer on Sandwich Complex for the Improvement of Sensitivity in Sandwich Enzyme-linked Immunoassay**

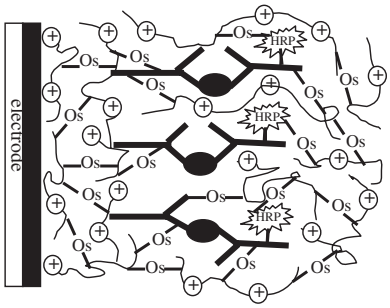

Qiang Gao, Bin Qi, Yufang Sha, and Xiurong Yang

1200 **Preparation of a Nanocrystalline TiO_2 Photocatalyst Using a Dry-process with Acetylene Black**

Weiping Tang, Zaihua Chen, and Shunsaku Katoh

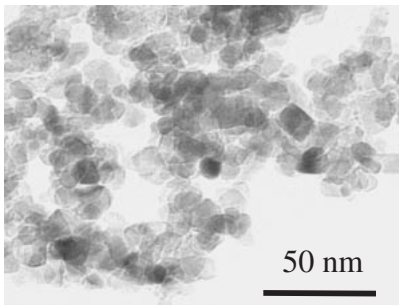

1202 **Artificial Assembly of Myoglobin and Flavodoxin Reductase Using Designed Coiled-coil Peptides**

Seiji Sakamoto, Atsushi Itoh, and Kazuaki Kudo

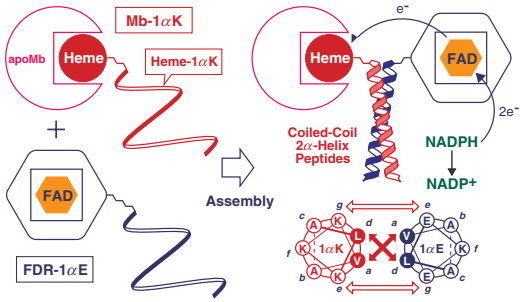

1204 **Biomimetic Hydrolysis of *p*-Nitrophenyl Alkanoates with Functionalized Mesoporous Silicas**

Jeong Ho Chang, Kyung Ja Kim, Young-Kook Shin, and Jun Liu

Hierarchically ordered nanoporous structure mimics an enzyme function as a chemical nanofactory ensemble. Biomimetic catalysis for *p*-nitrophenyl alkanoates as a function of alkanoate chain lengths was demonstrated with multifunctionalized nanoporous ceramic catalyst.

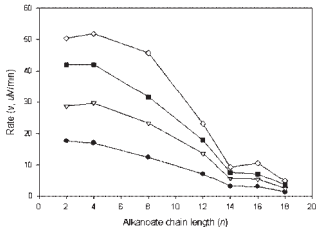

1206 **4-Difluoromethylated Quinoline Synthesis via Intramolecular S_N2' Reaction of α-Trifluoromethylstyrenes Bearing Imine Moieties**

Takashi Mori and Junji Ichikawa

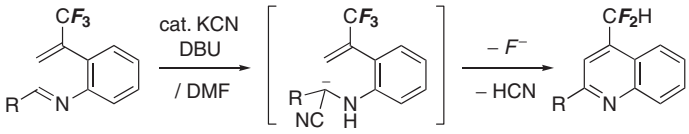

1208 **Novel Palladium Catalyst Supported on GaAs(001) Passivated by Ammonium Sulfide**

Ikuko Takamiya, Shiro Tsukamoto, Masahiko Shimoda, Naoki Miyashita, Mitsuhiro Arisawa, Yasuhiko Arakawa, and Atsushi Nishida

A highly reactive palladium catalyst for the Heck reaction supported on a sulfur-terminated GaAs(001) plate was developed. Sulfur termination using $(NH_4)_2S_x$ at 60 °C and Pd absorption in acetonitrile at 100 °C is essential for the preparation of an active and stable catalyst. The catalyst could be reused in this reaction up to ten times.

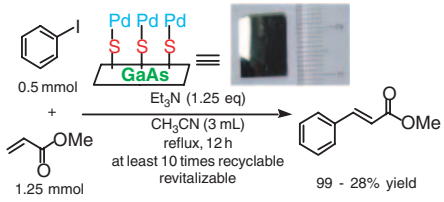

1210 **High Stability in Organic Solvent of Heme Proteins Immobilized in the Interlayers of Magadiite Nanoparticles**

Shuge Peng, Qiuming Gao, and Jianlin Shi

The first report of higher stability for heme proteins, Mb and Hb, immobilized in the interlayers of magadiite nanoparticles than that of free Mb and Hb in organic solvents.

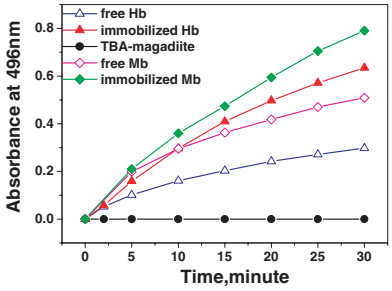

1212 **The First Enantiomerically Pure Synthesis of (*S*)- and (*R*)-Naftopidil Utilizing Hydrolytic Kinetic Resolution of (±)-(α-Naphthyl) Glycidyl Ether**

Kiran Kumar Kothakonda and D. Subhas Bose

Enatiomerically pure (*S*)-naphthyl glycidyl ether and (*R*)-1-naphthyl glycerol were prepared utilizing HKR ; opening of the pure terminal epoxide with 1-(2-methoxyphenyl) piperizine gave the enantiomerically pure (*S*)- and (*R*)-Naftopidil.

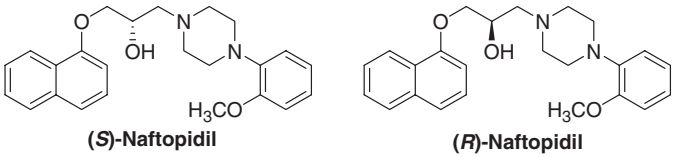

1214 **A Novel BEDT-TTF-based Organic Conducting Salt with a Ferrocene-containing Dianion, α-(BEDT-TTF)$_4$(Fe(Cp–CONHCH$_2$SO$_3$)$_2$)·4H$_2$O**

Keigo Furuta, Hiroki Akutsu, Jun-ichi Yamada, and Shin'ichi Nakatsuji

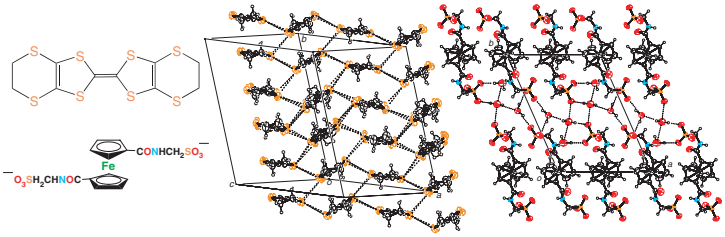

1216 **Photophysical and Photocatalytic Properties of Molybdates and Tungstates with a Scheelite Structure**

Hideki Kato, Naoko Matsudo, and Akihiko Kudo

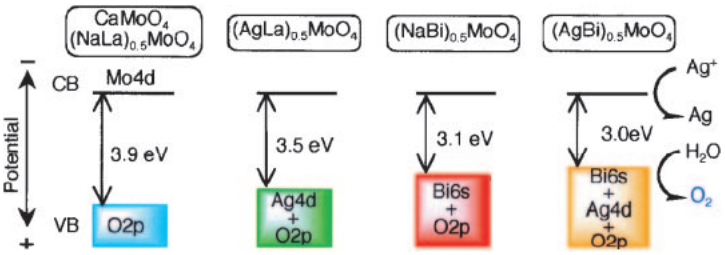

1218 **Synthesis of Novel Organic–Inorganic Hybrid Cages via Cobalt-catalyzed Cyclotrimerization of Dimethylethynylsilyl Groups on a Silsesquioxane**

Kenji Wada, Takuro Yamasaki, Teruyuki Kondo, and Take-aki Mitsudo

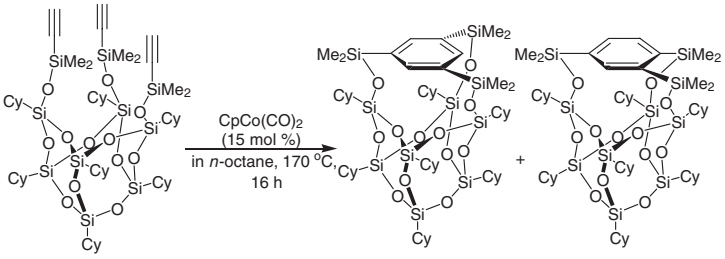

1220 **Hydrogen Adsorption/Desorption Property of Activated Carbon Loaded with Platinum**

Hideyuki Takagi, Hiroaki Hatori, and Yoshio Yamada

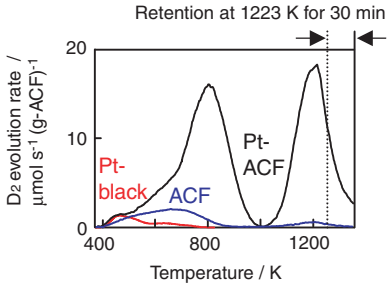

Two peaks in the D_2 desorption profile of Pt–ACF indicated that two kinds of sites for adsorption or bonding of spiltover deuterium exist on the carbon surface.

1222 **A Novel Enantioselective Reaction. Palladium-catalyzed Enantiodistinctive Reaction of Bicyclic Allylic Compounds**

Hisashi Daimon, Ryohei Ogawa, Shuichi Itagaki, and Isao Shimizu

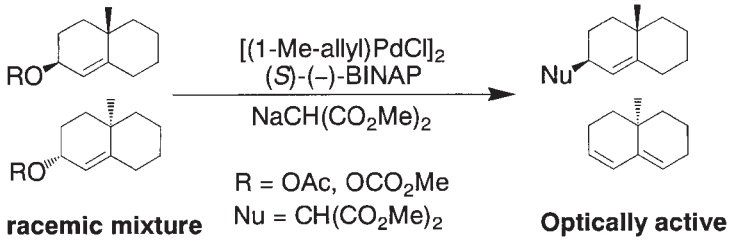

1224 **Wittig Type Methylenation of Ketones with Bis(iodozincio)methane and Ionic Liquid**

Hideaki Yoshino, Masami Kobata, Yuhei Yamamoto, Koichiro Oshima, and Seijiro Matsubara